

- ⁹J. M. Robinson and H. B. Gilbody, *Proc. Phys. Soc. (London)* **92**, 589 (1967).
- ¹⁰D. J. Baker, H. A. B. Gardiner, and J. J. Merrill, *J. Chim. Phys.* **64**, 63 (1967).
- ¹¹D. A. Dahlberg, D. K. Anderson, and I. E. Dayton, *Phys. Rev.* **164**, 20 (1967).
- ¹²E. W. Thomas, G. D. Bent, and J. L. Edwards, *Phys. Rev.* **164**, 32 (1968).
- ¹³H. A. B. Gardiner, J. J. Merrill, W. R. Pendleton, Jr., and D. J. Baker, *Appl. Opt.* **8**, 799 (1969).
- ¹⁴S. K. Allison and M. Garcia-Munoz, in *Atomic and Molecular Processes*, edited by D. R. Bates (Academic Press Inc., New York, 1962), p. 721.
- ¹⁵N. G. Utterback and T. Griffith, Jr., *Rev. Sci. Instr.* **37**, 866 (1966).
- ¹⁶J. D. Jobe, F. A. Sharpton, and R. M. St. John, *J. Opt. Soc. Am.* **57**, 106 (1967).
- ¹⁷J. W. McConkey, J. M. Woolsey, and D. J. Burns, *Planet. Space Sci.* **15**, 1332 (1967).
- ¹⁸E. S. Solov'ev, R. N. Il'in, V. A. Oparin, and N. V. Fedorenko, *Zh. Eksperim. i Teor. Fiz.* **42**, 659 (1962) [English transl.: *Soviet Phys. - JETP* **15**, 459 (1962)].
- ¹⁹G. Herzberg, *Ann. Physik* **86**, 189 (1928).
- ²⁰R. W. Nicholls, *J. Res. Natl. Bur. Std. (U.S.)* **65A**, 451 (1961).
- ²¹L. Wallace and R. W. Nicholls, *J. Atmos. Terr. Phys.* **7**, 101 (1955).
- ²²D. R. Bates and J. C. G. Walker, *Planet Space Sci.* **14**, 1367 (1966).
- ²³E. P. Wigner, *Nachr. Acad. Wiss. Gottingen Math. Physik Kl.* 375 (1927).
- ²⁴P. M. Stier and C. F. Barnett, *Phys. Rev.* **103**, 896 (1956).
- ²⁵D. J. Burns, F. R. Simpson, and J. W. McConkey, *J. Phys.* **B2**, 52 (1969).
- ²⁶B. N. Srivastava and I. M. Mirza, *Phys. Rev.* **168**, 87 (1968).

Total and Excitation-Transfer Cross Sections for Collisions between 2^3S Metastable and Ground-State Helium Atoms*

S. A. Evans[†] and Neal F. Lane[‡]

Department of Physics, Rice University, Houston, Texas 77001

(Received 7 July 1969)

Total and excitation-transfer cross sections for collisions between 2^3S metastable and ground-state helium atoms have been calculated in the perturbed-stationary-state approximation, using the best available adiabatic $^3\Sigma_u^+$ and $^3\Sigma_g^+$ potential curves for He_2 , and in the "diabatic" approximation, using a repulsive $^3\Sigma_g^+$ curve, constructed so as to have the appropriate united-atom limit. Both the total and excitation-transfer cross sections are found to show an oscillatory energy dependence. The detailed nature of these oscillations is found to be different for the adiabatic and "diabatic" descriptions. However, the average magnitude of the cross sections does not show this sensitivity. Differential cross sections have also been calculated and show considerable structure. Existing experimental measurements are included and compared with these calculations.

I. INTRODUCTION

The interaction between metastable and ground-state helium atoms has been of considerable interest to researchers for a long time. Starting with the suggestion by Nickerson,¹ that the existence of a diffuse 600 Å band in a helium discharge implied the existence of a maximum in the $^1\Sigma_u^+$ interaction potential, many experimental²⁻¹² and theoretical¹³⁻²¹ investigations have proceeded to demonstrate that maxima do exist in the interaction potentials (including nuclear repulsion) between metastable and ground-state helium atoms.

Since the original theoretical investigation of Buckingham and Dalgarno,¹⁴ many elaborate calculations have been carried out in which the $^1,^3\Sigma_g^+$ and $^1,^3\Sigma_u^+$ potentials, which arise from $2^1,^3S$ and 1^1S separated atoms, are all seen to possess potential maxima lying outside attractive potential wells.^{13,15-20} The maxima in the $^3\Sigma_g^+$ and $^1\Sigma_g^+$ curves apparently arise from avoided "crossings" with higher molecular states arising from the next highest separated-atom configuration.^{17,20,21} However, there is no current explanation of the maxima occurring in the $^3\Sigma_u^+$ and $^1\Sigma_u^+$ curves.²¹

The nature of the $^3\Sigma_g^+$ and $^3\Sigma_u^+$ molecular states

is of particular interest since the 2^3S atomic state of helium is highly metastable,²² and thus suitable for collisional studies in various types of experiments. Recently, Fitzsimmons, Lane, and Walters¹² measured the diffusion coefficient for 2^3S metastable helium atoms in ground-state helium gas over a wide range of temperatures from 1 to 300 °K. They used these results to construct semiempirical $^3\Sigma_u^+$ and $^3\Sigma_g^+$ potential curves at large separations. Having fixed the potentials in this manner, they then calculated total and excitation-transfer cross sections at thermal energies and found excellent agreement with the respective measurements of Rothe, Neynaber, and Trujillo²³ and Colegrove, Shearer, and Walters.¹⁰

In their paper, Fitzsimmons *et al.* have pointed out that the total and diffusion cross sections involve averages of cross sections associated with the *gerade* $V_g(R)$ and *ungerade* $V_u(R)$ interaction potentials, and are therefore insensitive to the precise form of the difference potential function $\Delta V(R) = V_g(R) - V_u(R)$. The excitation-transfer cross section is, however, sensitive to $\Delta V(R)$. They found that the parametrized form $\Delta V(R) = \gamma \exp(-\tau R)$, with $\gamma = 1.54$ a. u. and $\tau = 1.43a_0^{-1}$, was consistent with the difference between the $^3\Sigma_g^+$ curve of Greenawalt²⁰ and the $^3\Sigma_u^+$ curve of Matsen and Scott¹³ (both adjusted in the manner of Klein, Greenawalt, and Matsen¹⁹) over a limited region of R just outside the region of the potential maxima. The difference potential ΔV actually used by Fitzsimmons *et al.* in their calculation of the excitation-transfer cross section, however, has been found to be larger than that above by an additive term $2.93 \exp(-1.62R)$ a. u., and does result in excitation-transfer cross sections in good agreement with the low-energy measurement.¹⁰ This should be considered a minor correction to their paper since the determination of the long-range potentials using the diffusion measurements and the good agreement of the total cross sections with the measurements are not affected by this change in $\Delta V(R)$. In this paper, we will continue to use the long-range form for $\Delta V(R)$ given by Fitzsimmons *et al.* We will show, however, how a change in $\Delta V(R)$ of the magnitude mentioned above affects the cross sections.

The comparisons with thermal measurements are, however, only relevant to the long-range behavior of the interaction potentials, and the energies are so low that nonadiabatic effects are certainly expected to be negligible. In order to gain information about the short-range (i. e., region inside the repulsive maxima) dynamic interactions, comparisons must be made between laboratory measurements at higher energies and the results of theoretical investigations, carried out in such a way as to make clear the differences which result from alternative theoretical descriptions. We are most interested, for example, in deter-

mining where and in what manner the adiabatic approximation breaks down. At the same time we want to find out to what degree of validity the collision can be described by a pair of potential curves, adiabatic or otherwise. A complete quantum-mechanical treatment of the problem is, of course, very complicated. In the classic method of perturbed stationary states,²⁴⁻²⁶ one represents the time-independent wave function of the system as a superposition of adiabatic molecular electronic states, many of which are coupled in the collision problem by gradient-interaction terms. This coupling is particularly large near avoided crossings of the adiabatic curves and gives rise to transitions between electronic states. In cases where the coupling is strong, the adiabatic approximation, which consists of ignoring these gradient-interaction terms, should be expected to give poor results. Approximate methods to handle the "curve-crossing" problem were developed at a very early stage by Stueckelberg,²⁷ Landau,²⁸ and Zener²⁹; however, these methods are uncertain and subject to a variety of criticisms. Almost all calculations which involve coupling between electronic states have been carried out in the impact-parameter approximation,^{26,30-32} and consequently are reliable only at high energies.

An alternative approach to this type of scattering problem is the diabatic method of Lichten,³³⁻³⁵ in which curve crossings which would be forbidden in the Born-Oppenheimer approximation are allowed to occur in the collision problem. Thus, the collision is still described by well-defined potential curves; however, these are not the familiar Born-Oppenheimer adiabatic curves and their precise definition is open to some interpretation.³⁶ Applications of this method to the He-He⁺ problem, however, have been remarkably successful. Using this approach, Marchi and Smith³⁷ were able to reproduce the magnitude and many aspects of the structure in the differential cross sections observed by Lorentz and Aberth.³⁸ Slight adjustments of the He₂⁺ interaction potentials have been shown to yield even better agreement with the measurements.³⁹ Thus, while it must be said that the diabatic approach is not completely justified, it does, in some cases, appear to be a good description.

In the present paper, we give the results of calculations of the differential, total, and excitation-transfer cross sections for collisions between 2^3S metastable and ground-state helium atoms over a wide range of energies. Cross sections are obtained in both the adiabatic and diabatic approximations, and the differences are illustrated and discussed. In both descriptions, structure is observed in the energy dependence of the excitation-transfer and, to a lesser extent, in the total cross sections. The origin of this structure is discussed. Finally, comparisons are made with existing mea-

measurements of the excitation-transfer cross sections. At the time our results were first reported,⁴⁰ only preliminary measurements of the excitation-transfer cross section⁴¹ had been made, and these showed a smooth energy dependence. Refinements of these measurements have since verified the existence of structure. The details will be given later in the paper.

II. THEORY

The general formulation of the atom-atom collision problem may be found in the literature,^{24-36,42-44} and we will not attempt to repeat such a detailed description.

In the two-state approximation to the method of perturbed stationary states, the total wave function for the diatom He(2^3S)-He(1^1S) system may be written

$$\begin{aligned} \Psi(\vec{R}, \vec{r}_i) = & F_g(\vec{R}) \psi(^3\Sigma_g^+ | R, \vec{r}_i) \\ & + F_u(\vec{R}) \psi(^3\Sigma_u^+ | R, \vec{r}_i), \end{aligned} \quad (1)$$

where \vec{R} denotes the relative positions of the two atoms, and the ψ functions represent the electronic $^3\Sigma_g^+$ and $^3\Sigma_u^+$ state wave functions. The functions F_g and F_u describe the scattering state and, in cases where the R dependence of the electronic wave functions is weak, are taken to satisfy the uncoupled equations (atomic units are used throughout):

$$[\nabla_R^2 + k^2 - (2M)V_{g,u}(R)]F_{g,u}(\vec{R}) = 0, \quad (2)$$

where k^2 is related to the initial relative kinetic energy E_k by

$$k^2 = (2M)E_k, \quad (3)$$

and M is the reduced mass in atomic units. The interaction potentials are defined as

$$V_{g,u}(\vec{R}) = E_{g,u}(R) + 4/R - E(1^1S) - E(2^3S), \quad (4)$$

where $E_g(R)$ and $E_u(R)$ are the respective electronic energies of the $^3\Sigma_g^+$ and $^3\Sigma_u^+$ states of He₂, both of which asymptotically approach $E(1^1S) + E(2^3S)$, i. e., the sum of the atomic energies for the ground and 2^3S metastable states of helium. The required solutions of Eq. (1) have the asymptotic form

$$\begin{aligned} F_{g,u}(R) \sim & \alpha_{g,u} [\exp(ikZ) \\ & + R^{-1} \exp(ikR) f_{g,u}(\theta)], \end{aligned} \quad (5)$$

where the Z axis is taken along the direction of incidence of the 2^3S helium atom. Because of the indistinguishability of the helium nuclei, the correct wave function must be symmetric with respect to nuclear interchange (for He⁴). Thus Ψ in Eq. (1) is properly symmetrized, and the coefficients $\alpha_{g,u}$ chosen so as to yield a plane wave of 2^3S atoms incident along the Z axis. Massey and Smith²⁵ have treated this problem in detail and show that the total scattering amplitude is given by

$$\begin{aligned} F(\theta) = & 1/2[f_g(\theta) + f_u(\theta) \\ & + f_g(\pi - \theta) - f_u(\pi - \theta)]. \end{aligned} \quad (6)$$

Due to the forward peaking of $f_{g,u}(\theta)$ for most energies of interest, the first two terms dominate at small angles and are identified with direct elastic scattering while the last terms dominate for large angles and are interpreted as excitation transfer. The individual scattering amplitudes $f_{g,u}(\theta)$ may be represented in terms of a standard partial-wave expansion:

$$\begin{aligned} f_{g,u}(\theta) = & (2ik)^{-1} \sum_{l=0}^{\infty} [\exp(2i\eta_{g,u}^l) - 1] \\ & \times (2l+1)P_l(\cos\theta), \end{aligned} \quad (7)$$

where $\cos\theta = \hat{R} \cdot \hat{Z}$, and where the $\eta_{g,u}^l$ are scattering phase shifts associated with the potentials $V_{g,u}(R)$. The phase shifts are accurately determined, for the energies considered here, by the well-known semiclassical JWKB approximation,^{45, 46} where the phase shifts are given by

$$\begin{aligned} \eta_{g,u}^l = & \int_{R_0}^{\infty} [k^2 - (2M)V_{g,u}(R) - (l + \frac{1}{2})^2/R^2]^{1/2} dR \\ & - \int_{R_0'}^{\infty} [k^2 - (l + \frac{1}{2})^2/R^2] dR, \end{aligned} \quad (8)$$

with R_0 and R_0' the respective zeros of the integrands (outermost zero in the case of R_0); R_0 is often called the classical turning point or distance of closest approach.

The integrated total cross section may be expressed as

$$Q_T = Q_d + Q_t + Q_i, \quad (9)$$

where $Q_d = \frac{1}{2}\pi \int_0^\pi |f_g(\theta) + f_u(\theta)|^2 \sin\theta d\theta$

$$\begin{aligned} = & (\pi/k^2) \sum_{l=0}^{\infty} (2l+1) [2 \sin^2(\eta_g^l) \\ & + 2 \sin^2(\eta_u^l) - \sin^2(\eta_g^l - \eta_u^l)]; \end{aligned} \quad (10)$$

$$Q_t = \frac{1}{2}\pi \int_0^\pi |f_g(\pi - \theta) - f_u(\pi - \theta)|^2 \sin\theta d\theta$$

$$= (\pi/k^2) \sum_{l=0}^{\infty} (2l+1) \sin^2(\eta_g^l - \eta_u^l) \cong Q_T - Q_d; \quad (11)$$

and where Q_t is a cross term due to interference of direct and transfer scattering and is very small for all cases considered. The total differential scattering cross section is then given by

$$dQ_T(\theta)/d\Omega = |F(\theta)|^2 \quad (12)$$

and the differential transfer cross section by

$$dQ_t(\theta)/d\Omega = |F(\pi - \theta)|^2. \quad (13)$$

III. ADIABATIC INTERACTION POTENTIALS

The ${}^3\Sigma_g^+$ and ${}^3\Sigma_u^+$ interaction potentials, respectively denoted $V_g(R)$ and $V_u(R)$, have been the subject of several *ab initio* investigations, since Buckingham and Dalgarno¹⁴ first obtained a repulsive barrier in the $V_u(R)$ curve, lying outside the attractive region of the potential. These more recent investigations, involving much more elaborate variational calculations, have demonstrated that the "hump" is real^{13,15,16,19} and that the $V_g(R)$ curve possesses one as well.^{17,20} In the latter case, the hump arises from an avoided crossing of the ${}^3\Sigma_g^+$ curve corresponding to the separated-atom states He($1s^21^1S$) and He($1s2s2^3S$), and the adjacent ${}^3\Sigma_g^+$ curve just above, which corresponds to the separated atom states He($1s^21^1S$) + He($1s2p2^3P$). Repulsive barriers have also been predicted and found in several other excited states of He.^{21,47}

In the adiabatic calculations to be discussed here, we have used, for separations $R \lesssim 6a_0$, the ${}^3\Sigma_u^+$ curve of Matsen and Scott,¹³ as adjusted by Klein, Greenawalt, and Matsen¹⁹ and the ${}^3\Sigma_g^+$ curve of Greenawalt,²⁰ adjusted in the same manner. These curves were obtained by the standard variational method using, as a trial wave function, a linear combination of valence-bond single-configuration basis functions. The nonlinear parameters in the basis functions, as well as the linear coefficients, were varied at each internuclear separation. For larger separations, viz., $R > 6a_0$, it has been shown by Fitzsimmons, Lane, and Walters¹² that these potentials are consistently too large, in that they predict diffusion cross sections much larger than the measured values for temperatures of 1 to 300 °K. These authors suggest that a good representation of the interaction potentials for $R > 6a_0$ is given by

$$V_u(R) = \alpha R^2 e^{-\beta R},$$

$$V_g(R) = V_u(R) + \gamma e^{-\tau R}, \quad (14)$$

where $\alpha = 0.820$ a. u., $\beta = 1.6a_0^{-1}$, $\gamma = 1.54$ a. u. and $\tau = 1.43a_0^{-1}$. We have constructed analytic forms which reproduce the potentials of Matsen and Scott¹³ and Greenawalt²⁰ for small separations and go over smoothly to the semiempirical forms of Eqs. (14) for $R \gtrsim 6a_0$. These interactions are given in Fig. 1.

IV. PROCEDURE

The integrals involved in the JWKB approximation to the phase shifts [see Eq. (18)] were, in all cases, evaluated with a sixth-order quadrature formula. A step size of $0.01a_0$ was always sufficient to limit errors in the integration to less than 0.3%. Phase shifts calculated in this way were, for a variety of values of l and k , compared with the results of a direct numerical solution of the differential Eq. (2), using the Numerov method.⁴⁸ Except for cases involving classical "orbiting,"⁴⁶ the phase shifts determined in these two ways were in excellent agreement. For the energies of principal interest here, say $E \gtrsim 0.1$ eV ($k \gtrsim 5.19$), the JWKB method is found to be very good.

The total cross section Q_T and the excitation-transfer cross section Q_t were calculated according to Eqs. (9)–(11). The phase shifts were calculated at convenient intervals in l , and a five-point interpolation was used to obtain all the remaining values necessary for evaluation of the summations. In the energy range $0.37 \leq E \leq 2.3$ eV, the interpolation became inaccurate due to the strong l dependence of the phase shifts, and it was necessary to calculate each phase shift directly. In the calculation of the transfer cross section Q_t of Eq. (11), the necessary phase shifts were also determined either directly or by inter-

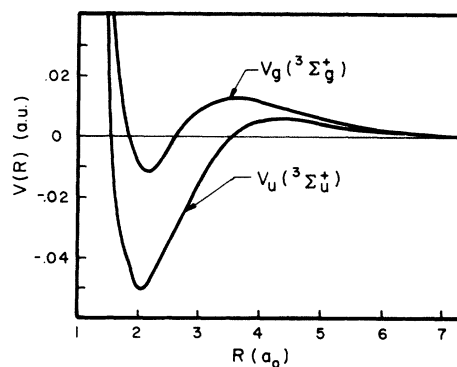


FIG. 1. Adiabatic ${}^3\Sigma_g^+$ and ${}^3\Sigma_u^+$ interaction potentials (Refs. 13, 19, and 20) between ground-state and 2^3S metastable helium atoms.

polation and the summation carried out term by term. Differential cross sections were calculated using Eqs. (12) and (13). All procedures and computer codes were checked by repeating the calculations of Marchi and Smith on total scattering of He^+ by He, using interaction potentials given by these authors.³⁷

We shall first discuss cross sections obtained using the adiabatic ${}^3\Sigma_u^+$ and ${}^3\Sigma_g^+$ interaction potentials discussed above. Next, we will indicate how the total and transfer cross sections respond to small changes in the adiabatic curves. Finally, we will discuss the behavior of cross sections corresponding to a diabatic picture in which a *gerade* potential is constructed which qualitatively represents a crossing situation and is repulsive at all separations.

V. COLLISION ON ADIABATIC INTERACTION POTENTIAL CURVES

The total cross section of Eq. (9) may be considered an average of elastic cross sections defined for the g and u curves separately, viz.,

$$Q_T = 1/2(Q_g + Q_u), \quad (15)$$

$$\text{where } Q_{g,u} = \frac{4\pi}{k^2} \sum_{l=0}^{\infty} (2l+1) \sin^2(\eta_{g,u}^l).$$

In Figs. 2 and 3 are plotted curves for Q_g , Q_u , and Q_T as functions of energy. The total cross section at thermal energies is completely determined by the long-range interaction of Eqs. (14) and is in good agreement with the measurements of Rothe, Neynaber, and Trujillo²³ as discussed elsewhere.¹² The cross sections all vary smoothly for energies less than about 0.15 eV for Q_u and 0.35 eV for Q_g , above which oscillations set in. These energies correspond to the barrier heights of the two potential curves. If the true barriers are indeed smaller, as has been suggested by other investigators,⁴⁹ one may expect

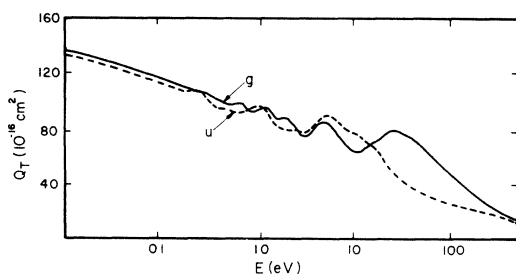


FIG. 2. Total cross sections Q_g and Q_u calculated in the adiabatic approximation.

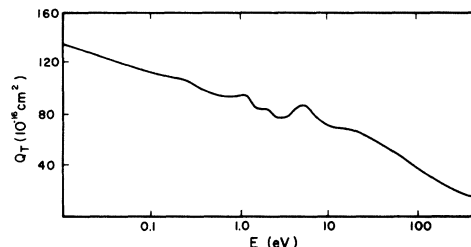


FIG. 3. Total cross section in the adiabatic approximation.

oscillations to set in at even lower energies. In order to illustrate how these oscillations arise, we will compare the scattering phase shifts at energies corresponding to relative maxima and minima in the cross sections. In Figs. 4 and 5 are plotted phase shifts η_g^l and η_u^l as functions of l for the two energies 5.95 and 11.2 eV, corresponding, respectively, to a relative maximum and minimum in Q_g . It is seen that the variation in l of the negative phase shifts $-\eta_{g,u}^l$ closely resembles the variation in R of the respective interaction potentials, including the minimum and maximum. For relatively small values of l , away from the maxima or minima in the $-\eta_{g,u}^l$ curves, the phase shifts are rapidly varying with l , and contributions to the cross sections $Q_{g,u}$ may be well represented by the random-phase approximation, where $\sin^2 \eta_{g,u}^l$ in Eq. (15) is replaced by its average value of $\frac{1}{2}$ for all l values in this range of rapid variation. The energy variation of these contributions is smooth and therefore is not associated with the structure. Values of l in the vicinity of the maxima and minima in the $-\eta_{g,u}^l$ curves do not, however, make random contributions to the cross sections,

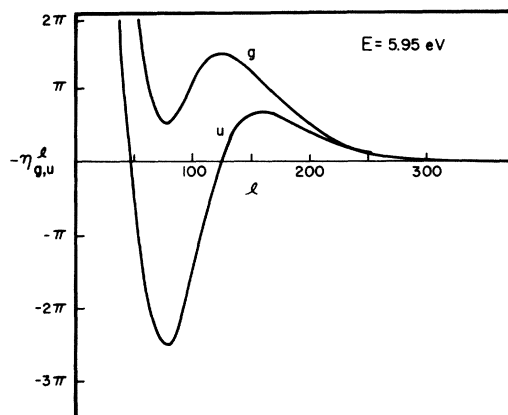


FIG. 4. Phase shifts for *gerade* and *ungerade* scattering at 5.95 eV (adiabatic approximation).

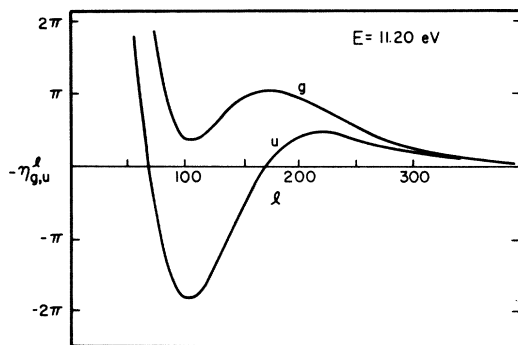


FIG. 5. Phase shifts for *gerade* and *ungerade* scattering at 11.2 eV (adiabatic approximation).

since the variation of the $\eta_{g,u}^l$ with l is slow and many phase shifts in this region make similar contributions. If the interaction potentials are strong enough, a variation in energy may take the maximum or minimum phase shifts through series of even and odd multiples of $\frac{1}{2}\pi$, giving rise to an oscillatory contribution to the cross sections from these values of l . This type of structure is present in cross sections associated with a large number of atomic systems and, in cases involving a single interaction potential, the number of maxima observed can be taken as a measure of the number of bound vibrational states in the diatom system.⁵⁰ In the present case, the presence of potential maxima makes the structure somewhat more complicated.

In Fig. 4, we see that at 5.95 eV $-\eta_g^l$ has a relative minimum value of $\approx \frac{1}{2}\pi$ at $l \approx 75$, and a maximum of $\approx \frac{3}{2}\pi$ at $l \approx 120$. Thus, we expect a rather large nonrandom contribution to Q_g . This is indeed seen to be the case in Fig. 6, which shows the partial-wave contributions to Q_g for 5.95 eV. At 11.2 eV, however, we see in Fig. 5 that $-\eta_g^l$ has a relative minimum value just under $\frac{1}{2}\pi$ at $l \approx 110$ and a maximum of $\approx \pi$ at $l \approx 170$, which in-

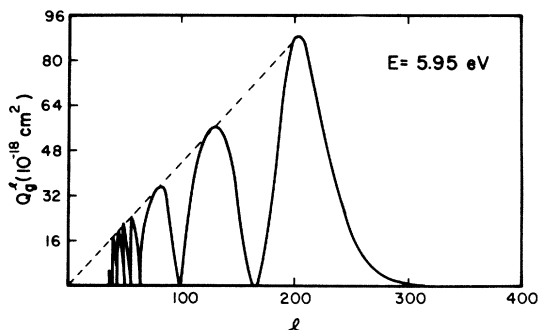


FIG. 6. Partial-wave contributions to the total *gerade* cross section Q_g at 5.95 eV (adiabatic approximation).

dicates a rather small nonrandom contribution to Q_g . This is easily seen in Fig. 7, where l values in the range 160 to 200 are found to make essentially no contribution to Q_g . The *ungerade* phase shifts are found to make rather similar contributions to Q_u for the lower energy of 5.95 eV. However, at 11.2 eV, the minimum value of $-\eta_u^l$, which occurs for $l \approx 100$, is just above -2π , while the maximum, occurring for $l \approx 220$, is very close to $\frac{1}{2}\pi$. Thus, these nonrandom contributions tend to cancel, and we have no well-defined minimum in Q_u at $E = 11.2$ eV. This type of interference between the regions of phase-shift maximum and minimum results in an irregular structure in the individual curves for Q_g and Q_u . Thus, the total cross section Q_T shows an irregular energy dependence as compared with the smooth undulations commonly observed in cross sections for other systems. At somewhat higher energies, the phase shifts become smaller, and more slowly varying in energy, and the structure disappears.

For energies in the range of about 0.09 to 5.9 eV the phase shifts are found to possess discontinuities in l due to the phenomenon of classical orbiting.⁴⁶ This may be easily illustrated by considering the first integrand in the JWKB formula for the phase shifts given in Eq. (8). For l values not too large, the "effective" potential

$$V_{\text{eff}}(R) = (2M/m)V_{g,u}(R) + (l + \frac{1}{2})^2/R^2 \quad (16)$$

possesses a maximum which increases with increasing l . For a given energy, (i. e., k^2) it is possible to find two adjacent values of l such that the smaller is associated with a small turning point R_0 (i. e., classically, the particle passes over the barrier) and the larger, a large turning point (classically, the particle is turned back by the outer barrier). This discontinuous behavior in R_0 is, of course, reflected in the phase shifts. A typical case is illustrated in Fig. 8 for an energy of 0.182 eV. We have also calculated the

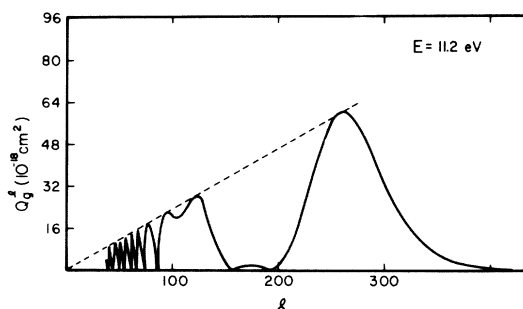


FIG. 7. Partial-wave contributions to the total *gerade* cross section Q_g at 11.2 eV (adiabatic approximation).

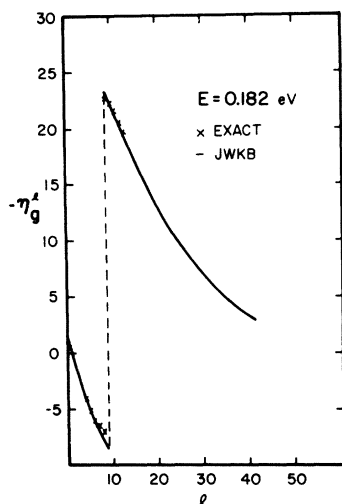


FIG. 8. Comparison of JWKB and exact *gerade* phase shifts at 0.182 eV in a region of orbiting (adiabatic approximation).

phase shifts at this energy by numerically solving the differential equations of Eq. (2). These values are also given for comparison. The deBroglie wavelength is about $0.9a_0$ for this energy, and the error in the JWKB approximation is seen to be small except in the immediate vicinity of the orbiting value of the angular momentum. The resulting error in the cross sections is very small.

The excitation-transfer cross section Q_t^l of Eq. (11) is plotted in Fig. 9 as a function of energy. These cross sections were calculated using "adiabatic" interaction potentials. The solid curve corresponds to use of the adiabatic interaction potentials of Eqs. (14). The dashed curve shows the effect of increasing the long-range difference between the *gerade* and *ungerade* potentials by an additive term of the form $2.93 e^{-1.62R}$ a. u. in the region $R \gtrsim 6a_0$, and zero elsewhere. As

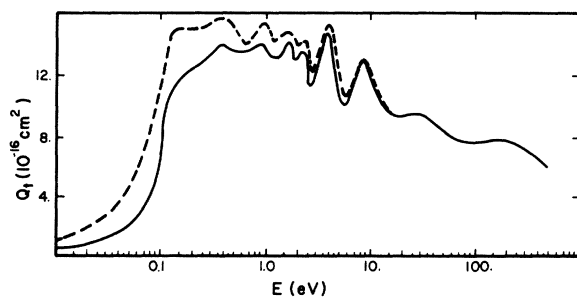


FIG. 9. Excitation-transfer cross section (adiabatic approximation). Solid curve corresponds to the long-range behavior of the potentials given by Eq. (27). Dashed curve corresponds to a somewhat larger differential potential as discussed in the text.

mentioned earlier, this somewhat larger difference potential is the form actually used by Fitzsimmons *et al.*¹² and is in good agreement with the low-energy measurements.¹⁰ We will, however, continue to use the long-range difference potential of Eqs. (14) throughout this paper.

The energy dependence of Q_t^l is also seen to possess considerable structure for energies sufficient to "clear" the barriers in the interaction potentials. For energies between 5.9 and 9.3 eV, Q_t^l increases from a minimum value of $10 \times 10^{-16} \text{ cm}^2$ to a maximum value of $13.4 \times 10^{-16} \text{ cm}^2$, a change of about 25%. In order to illustrate how this structure arises, we have plotted in Fig. 10 the phase differences $|\eta_g^l - \eta_u^l|$ versus l for several energies. Referring back to Eq. (11), we note that the partial-wave contributions to Q_t^l are given by

$$Q_t^l = (\pi/k^2) (2l+1) \sin^2(\eta_g^l - \eta_u^l).$$

In the energy range 4.55 to 13.35 eV, the phase-difference curves are flat for small values of l and roughly 100 partial waves contribute equally to Q_t^l . This contribution is small, for example, at 5.95 eV, where the phase differences are of the order 3π , but somewhat larger for 8.55 eV, where the phase differences are close to $\frac{5}{2}\pi$, especially for values of l between, say, 75 and 100. Thus, at these lower energies, the contribution to Q_t^l from, say, $l \lesssim 100$ oscillates with energy. The contribution from larger values of l varies much more smoothly with energy and constitutes the "background" on which the oscillatory part rides. The partial-wave contributions Q_t^l for these two energies are given in Fig. 11. The classical

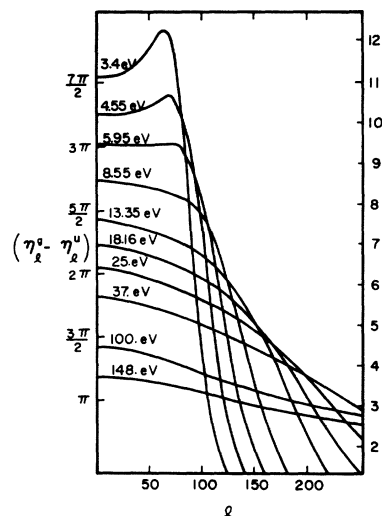


FIG. 10. Differences in *gerade* and *ungerade* phase shifts for several energies (adiabatic approximation).

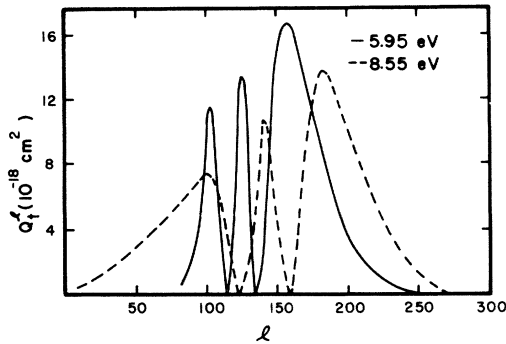


FIG. 11. Partial-wave contributions to the excitation transfer cross section at 5.95 and 8.55 eV (adiabatic approximation).

turning points R_0 of Eq. (8) associated with the *gerade* potential at these energies range from about $1.3a_0$ ($l=0$) and $2.5a_0$ ($l=100$) at 5.95 eV to $1.2a_0$ ($l=0$) and $2.0a_0$ ($l=100$) at 8.55 eV; the turning points for the *ungerade* potential are comparable. Thus, referring to the interaction potentials in Fig. 1, we note that the oscillatory contribution to Q_t arises primarily from scattering inside the region of the potential barriers, and we should expect the structure in Q_t to be rather insensitive to modifications of the interaction potentials in the region of the barriers.

The smoothly varying background contribution to Q_t , which is always much larger than the oscillatory part, arises primarily from outer regions of the interaction potentials. In particular, referring to Fig. 10, for the energies 5.95 and 8.55 eV we consider contributions from, say, $l > 100$ as comprising the background. The turning points associated with the *gerade* potential at these energies are in the range $2.5a_0$ ($l=100$) to $5a_0$ ($l=200$) for 5.95 eV and $2.0a_0$ ($l=100$) to $4a_0$ ($l=200$) for 8.55 eV. Again, the *ungerade* turning points are comparable. Thus, in this middle range of energies we expect the average magnitude of the transfer cross section to be most sensitive to the details of the interaction potentials in the region of the barriers, while the structure itself should depend primarily on the short-range nature of the potentials.

In order to examine the sensitivity of the transfer cross section to variations in the interaction potentials, we have carried out calculations for several modifications of the adiabatic interaction potentials. The results are given in Fig. 12, where the labels Aa, Ba, \dots refer to different combinations of *gerade* (A, B, \dots) and *ungerade* (a, b, \dots) potential curves as defined in Fig. 13. Thus the cross sections labeled Aa refer to the unmodified adiabatic potentials we have been discussing all along. A comparison of the transfer cross sections corresponding to these modified interaction

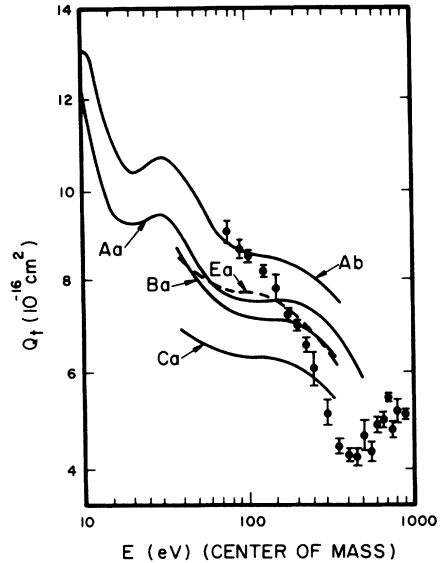


FIG. 12. Comparison of excitation-transfer cross sections for several choices of *gerade* (capital letters) and *ungerade* (small letters) interaction potentials as illustrated in Fig. 13. The closed circles refer to the measurements of Ref. 41.

potentials indicates that the magnitude of the cross section is rather sensitive to the difference between the *gerade* and *ungerade* potentials in the region of the barriers, while the amplitude and frequency of the oscillations remain much the same. Measurements of the deactivation cross section for 2^3S metastable helium in collision with ground-state atoms have been carried out by Sheridan, Peterson, Hollstein, and Lorentz.⁴¹ Their results may be compared directly

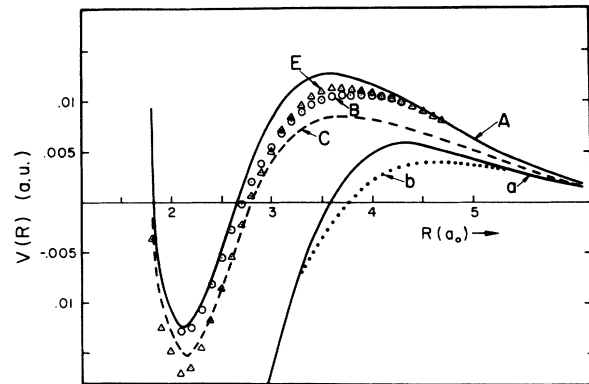


FIG. 13. Comparison of different *gerade* (capital letters) and *ungerade* (small letters) interaction potentials referred to in Fig. 12. The combination Aa represents the theoretical adiabatic curves (Refs. 13, 19, and 20) already discussed and illustrated in Fig. 1.

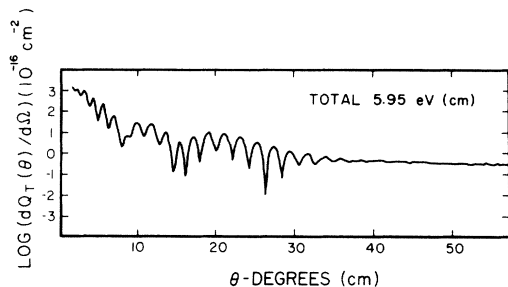


FIG. 14. Differential total cross section at 5.95 eV (center of mass) versus scattering angle (center of mass).

with Q_t and are included in Fig. 12. The comparison suggests that if the collision is in fact primarily elastic and nearly adiabatic, so that use of adiabatic interaction potentials and the neglect of higher excited states are justified, then the correct *gerade* and *ungerade* potentials must, in fact, be of a rather different form from the modified and unmodified curves we have used here. Differential cross sections have also been calculated using the theoretical adiabatic curves Aa , and the results are given in Figs. 14–19 for energies 5.95–300 eV.

VI. COLLISION ON DIABATIC INTERACTION POTENTIAL CURVES

In Sec. V, we have discussed the characteristics of the total and transfer cross sections one should expect under adiabatic conditions, i. e., when the nonadiabatic interaction matrix elements are neglected, so that the collision can be described as occurring on ordinary Born-Oppenheimer potential curves. These nonadiabatic coupling matrix elements are difficult to calculate and, at the present time, the magnitude and R dependence of these matrix elements remains unknown, although one expects maxima in this coupling in the vicinity of avoided crossings of the adiabatic potential curves. The diabatic description^{33–35} of a collision essen-

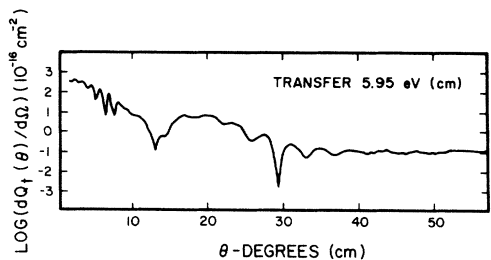


FIG. 15. Differential excitation-transfer cross section at 5.95 eV.

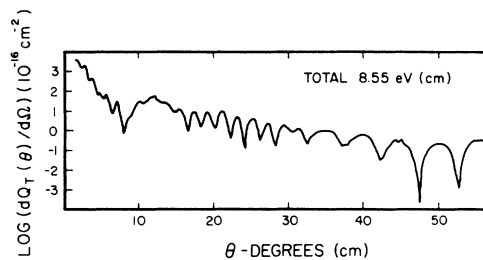


FIG. 16. Differential total cross section at 8.55 eV.

tially presupposes that the nonadiabatic coupling is dominant, so that in the vicinity of an avoided crossing of adiabatic potential curves, the system jumps with high probability onto the adjacent curve and continues on to the next avoided crossing, where it jumps again. Thus, the collision process appears to proceed as if the system were accurately described by some kind of potential curve (diabatic curve) which freely crosses adiabatic curves of like symmetry and quantal description.³⁶

The idea of a diabatic description may be invoked at the molecular orbital level, where the nonadiabatic interaction allows curve crossings which are forbidden in the adiabatic approximation by the famous noncrossing rule of Von Neumann and Wigner.⁵¹ This avoided crossing of molecular-orbital energy curves may be thought of as due to the incomplete screening of the nuclei by other electrons in the molecule.³⁵ The crossing versus avoided crossing of molecular orbital energy curves is *not* a problem with states arising from $1s$ or $2s$ separated atomic orbitals, and thus does not concern us directly in the study of collision between 2^3S and 1^1S ground-state helium atoms. Curve crossing or avoided crossing may also be discussed at the level of many-electron molecular states, where electronic energy curves of like symmetry and quantal description repel each other through configuration interaction, and thus avoid crossing in the Born-Oppenheimer approximation. Thus, for example, we often find cases where, at

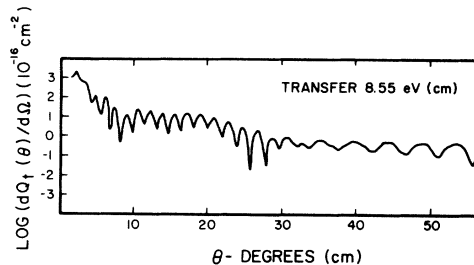


FIG. 17. Differential excitation-transfer cross section at 8.55 eV.

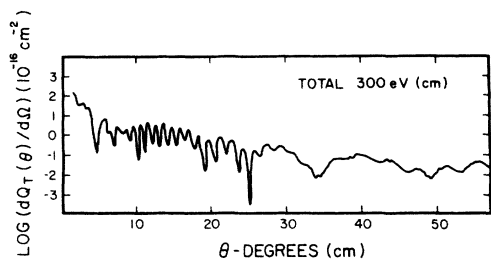


FIG. 18. Differential total cross section at 300 eV.

a particular separation (say, $R=R_c$), two single-configuration molecular-orbital energy curves cross. If, however, one considers the interaction of these two configurations by solving the appropriate 2×2 secular equation, new wave functions and electronic energy curves are obtained which do not cross at R_c , and one speaks of an avoided crossing of these configuration-interaction energy curves. The nonadiabatic coupling terms, which are ignored in the Born-Oppenheimer approximation, allow the system to jump from one curve to the next in spite of the avoided crossing of the adiabatic curves. When these nonadiabatic terms are dominant we speak of a diabatic interaction, and the system appears to be described by a potential curve which freely crosses adiabatic curves regardless of their quantal nature. This diabatic description has been extremely successful in treating scattering between He^+ ions and He atoms over a wide range of energies from about 15 eV upwards.³⁷

For collisions with helium in the 2^3S metastable ground state, the scattering state is described by a superposition of *gerade* and *ungerade* molecular states, $\psi(^3\Sigma_g^+)$ and $\psi(^3\Sigma_u^+)$, which at large separations may be associated with properly symmetrized linear combinations of separated-atom product functions of the form $1s_a(1)\bar{1}s_a(2)1s_b(3) \times 2s_b(4)$. Figure 20 contains a schematic diagram of a few of the separated- and united-atom energy levels associated with $^3\Sigma$ states of the He_2 system. States at intermediate separations are indicated by solid (configuration-interaction) and

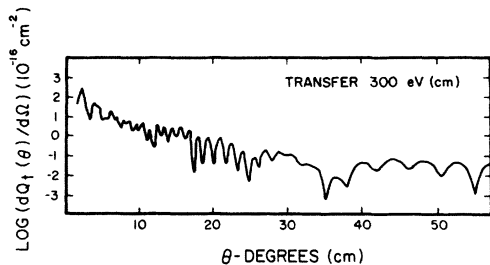
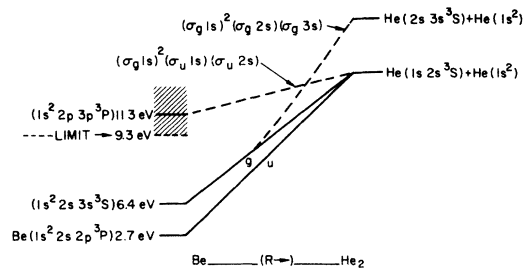


FIG. 19. Differential excitation-transfer cross section at 300 eV.

FIG. 20. Correlation diagram for selected states of the He_2 molecule to illustrate the adiabatic (solid lines) and diabatic (broken lines) descriptions.

dashed (single-configuration) lines. The $^3\Sigma_u^+$ state arising from $\text{He}(1^1\text{S}) + \text{He}(2^3\text{S})$ is dominated in the region of interaction by the single configuration $(1s\sigma)^2(2s\sigma)(2p\sigma)$ which is not crossed by any other configuration. Thus there is no avoided crossing associated with this lowest $^3\Sigma_u^+$ adiabatic state of He_2 (lowest solid line in Fig. 10), and its description is unambiguous. In the case of the $^3\Sigma_g^+$ state the situation is rather different. At large separations, the configuration $(\sigma_g 1s)^2 \times (\sigma_u 1s)(\sigma_u 2s)$, which correlates with $(1s\sigma)^2(2p\sigma) \times (3p\sigma)$, plays a major role. However, at about $R=3a_0$, a crossing occurs with $(\sigma_g 1s)^2(\sigma_g 2s)(\sigma_g 3s)$, which correlates with $(1s\sigma)^2(2s\sigma)(3s\sigma)$, and at still smaller separations the latter configuration dominates the adiabatic $^3\Sigma_g^+$ state. (These two configurations are represented by dashed lines in Fig. 20.) A diabatic description of this problem would, by analogy to the $\text{He}^+ - \text{He}$ collision problem, correspond to describing the $^3\Sigma_g^+$ state by the single configuration $(1s\sigma)^2(2p\sigma)(3p\sigma)$ at small separations and ignoring the interaction with $(1s\sigma)^2(2s\sigma)(3s\sigma)$ at the crossing. We have constructed a diabatic $^3\Sigma_g^+$ electronic energy curve by joining a smoothly varying analytic form to the adiabatic $^3\Sigma_g^+$ curve outside the crossing. The united atom energy is set at about 8.6 eV above the $1s^2 2s 2p^3 P$ state of Be; this corresponds approximately to the energy of the $1s^2 2p 3p$ configuration of Be. The resulting diabatic $^3\Sigma_g^+$ potential energy curve, obtained by adding on the internuclear repulsion $4/R$, is repulsive at all separations and is compared with the adiabatic curve in Fig. 21. The diabatic curve is labeled *D*.

Total and excitation-transfer cross sections have been calculated using this diabatic $^3\Sigma_g^+$ curve, along with the adiabatic $^3\Sigma_u^+$ curve, denoted as curve *a*. In Fig. 22, the resulting total cross section is compared with the adiabatic results discussed earlier. The average magnitude of the cross section is much the same; however, the structure is somewhat different. In the diabatic case, the *gerade* contribution to the cross section varies smoothly with energy, since it arises from

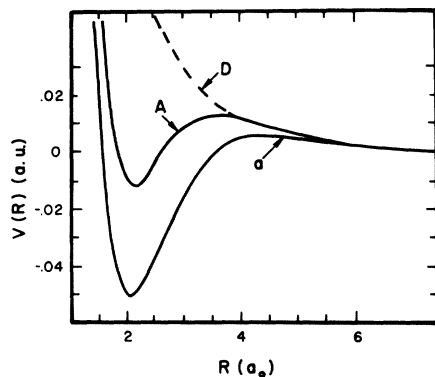


FIG. 21. Comparison of adiabatic (*A*) and diabatic (*D*) gerade interaction potential curves. The ungerade curve (*a*) is also given.

a completely repulsive potential. Thus, the oscillations in the total cross section are due entirely to ungerade scattering, and thus are identical to what we obtained earlier for Q_u .

In Fig. 23, the diabatic excitation-transfer cross section, labeled *Da*, is compared with the adiabatic cross section denoted by *Aa*. Again, the average magnitudes of the two cross sections are quite close while the detailed structure is different, the oscillations in the diabatic case being of somewhat higher frequency. This is all consistent with our earlier remarks to the effect that details of the structure are most sensitive to the short-range behavior of the interaction potentials, while the average magnitude of the transfer cross section depends on the potentials in the vicinity of the barriers. The experimental deactivation cross section data⁴¹ are also given in Fig. 23. The measurements do show the presence of some structure; however, the detailed energy dependence does not agree with the calculations.

VII. SUMMARY AND CONCLUSIONS

The total and excitation-transfer scattering of 2^3S metastable helium atoms on ground-state helium atoms has been discussed from the two different points of view, corresponding to the adiabatic and diabatic approaches. Total and transfer cross sections have been calculated and compared over a wide range of energy. The structure, found to be present in both total and transfer cross sections, has been shown to be directly related to the detailed behavior of the interaction potentials. The average magnitude of the transfer cross section is found to be particularly sensitive to the potentials in the vicinity of the barrier. Therefore, even within the adiabatic approximation, one will expect the magnitude of the transfer cross section to be somewhat different

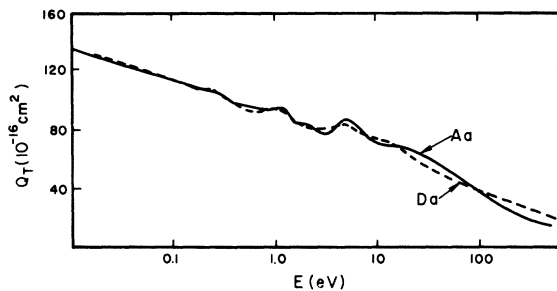


FIG. 22. Comparison of total scattering cross sections in the adiabatic (*Aa*) and diabatic (*Da*) approximations.

if more accurate adiabatic potential curves are used. In comparing transfer cross sections resulting from these two approaches, we have found that the major differences lie in the general character of the oscillatory contributions to the cross sections. The frequencies associated with the diabatic approach are larger and the amplitudes smaller than the adiabatic results. The experimental measurements verify the presence of structure in the excitation-transfer cross section.

ACKNOWLEDGMENTS

The authors are grateful to R. E. Olson and J. R. Peterson for many helpful comments and suggestions concerning the manuscript, and to A. Dalgarno, J. C. Browne, and F. T. Smith for

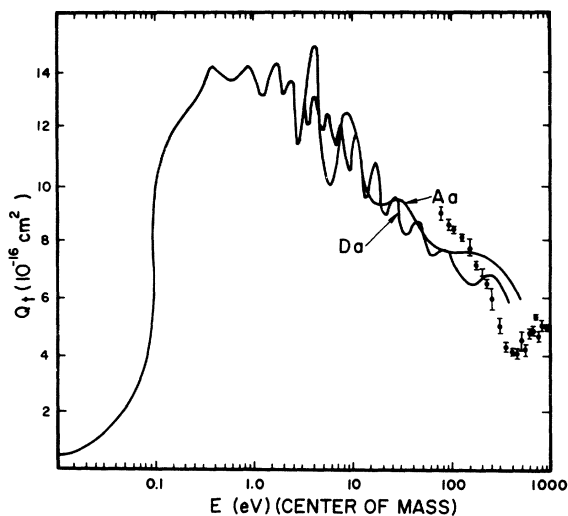


FIG. 23. Comparison of excitation-transfer cross sections in the adiabatic (*Aa*) and diabatic (*Da*) approximations. The measurements (Ref. 41) are given in the closed circles.

stimulating discussions. We also wish to thank E. M. Greenawalt for sending his potential curve prior to publication; and J. R. Sheridan, J. R.

Peterson, M. Hollstein, and D. C. Lorentz for allowing us to include their experimental results prior to publication.

* Research supported in part by the U. S. Atomic Energy Commission.

† National Science Foundation Fellow.

‡ Alfred P. Sloan Foundation Fellow.

¹J. L. Nickerson, *Phys. Rev.* **47**, 707 (1935).

²E. Ebbinghaus, *Ann. Phys. (N. Y.)* **7**, 267 (1930).

³M. A. Biondi, *Phys. Rev.* **88**, 660 (1952).

⁴A. V. Phelps and J. B. Molnar, *Phys. Rev.* **89**, 1202 (1953).

⁵E. H. S. Burhop, *Proc. Phys. Soc. (London)* **A67**, 276 (1954).

⁶A. V. Phelps, *Phys. Rev.* **99**, 1307 (1955).

⁷E. E. Benton, E. E. Ferguson, F. A. Matsen, and W. W. Robertson, *Phys. Rev.* **127**, 206 (1962).

⁸Y. Tanaka and K. Yoshino, *J. Chem. Phys.* **39**, 3081 (1963).

⁹E. E. Muschlitz and H. L. Richards, *J. Chem. Phys.* **41**, 559 (1964).

¹⁰F. D. Colegrove, L. D. Shearer, and G. K. Walters, *Phys. Rev.* **135**, 353 (1964). See also, H. J. Kolker and H. H. Michels, *J. Chem. Phys.* **50**, 1762 (1969).

¹¹K. H. Ludlum, L. P. Larson, and J. M. Caffrey, Jr., *J. Chem. Phys.* **46**, 127 (1967).

¹²W. A. Fitzsimmons, N. F. Lane, and G. K. Walters, *Phys. Rev.* **174**, 193 (1968). See also, I. Ya Fugol' and P. L. Pakhomov, *Zh. Eksperim. i Teor. Fiz.* **53**, 866 (1967) [English transl.: *Soviet Phys. - JETP* **26**, 526 (1968)].

¹³F. A. Matsen and D. R. Scott, in *Quantum Theory of Atoms, Molecules, and the Solid State*, edited by P. -O. Löwdin (Academic Press Inc., New York, 1966), p. 133.

¹⁴R. A. Buckingham and A. Dalgarno, *Proc. Roy. Soc. (London)* **A213**, 327 (1952).

¹⁵G. H. Brigman, S. J. Brient, and F. A. Matsen, *J. Chem. Phys.* **34**, 958 (1961).

¹⁶R. D. Poshusta and F. A. Matsen, *Phys. Rev.* **132**, 307 (1963).

¹⁷J. C. Browne, *J. Chem. Phys.* **42**, 2826 (1965).

¹⁸D. R. Scott, E. M. Greenawalt, J. C. Browne, and F. A. Matsen, *J. Chem. Phys.* **44**, 2981 (1966).

¹⁹D. J. Klein, E. M. Greenawalt, and F. A. Matsen, *J. Chem. Phys.* **47**, 4820 (1967).

²⁰E. M. Greenawalt, Ph.D. thesis, University of Texas, 1967 (unpublished).

²¹R. S. Mulliken, *Phys. Rev.* **136**, A962 (1965).

²²J. S. Mathis, *Astrophys. J.* **125**, 318 (1957).

²³E. W. Rothe, R. H. Neynaber, and S. M. Trujillo, *J. Chem. Phys.* **42**, 3310 (1965).

²⁴N. F. Mott and H. S. W. Massey, *The Theory of Atomic Collisions* (Oxford University Press, London, 1965), 3rd ed., p. 428; 2nd ed., p. 153.

²⁵H. S. W. Massey and R. A. Smith, *Proc. Roy. Soc.*

(London) **A142**, 142 (1933).

²⁶D. R. Bates, H. S. W. Massey, and A. L. Stewart, *Proc. Roy. Soc. (London)* **A216**, 437 (1953).

²⁷E. C. G. Stueckelberg, *Helv. Phys. Acta* **5**, 370 (1932).

²⁸L. Landau, *Physik. Z. Sowjetunion* **2**, 46 (1932).

²⁹C. Zener, *Proc. Roy. Soc. (London)* **A137**, 696 (1932).

³⁰N. F. Mott, *Proc. Cambridge Phil. Soc.* **27**, 553 (1931).

³¹D. R. Bates, in *Atomic and Molecular Processes*, edited by D. R. Bates (Academic Press Inc., New York, 1962), p. 550.

³²D. R. Bates and D. A. Williams, *Proc. Phys. Soc. (London)* **83**, 425 (1964); L. Wilets and D. F. Gallaher, *Phys. Rev.* **147**, 13 (1966).

³³W. Lichten, *Phys. Rev.* **131**, 229 (1963).

³⁴W. Lichten, *Phys. Rev.* **139**, A27 (1965).

³⁵W. Lichten, *Phys. Rev.* **164**, 131 (1967).

³⁶T. F. O'Malley, *Phys. Rev.* **162**, 98 (1967); F. T. Smith, *ibid.* **179**, 111 (1969).

³⁷R. P. Marchi and F. T. Smith, *Phys. Rev.* **139**, A1025 (1965).

³⁸D. C. Lorents and W. Aberth, *Phys. Rev.* **139**, A1017 (1965).

³⁹R. E. Olson and C. R. Mueller, *J. Chem. Phys.* **46**, 3810 (1967).

⁴⁰S. A. Evans and N. F. Lane, *Bull. Am. Phys. Soc.* **14**, 262 (1969).

⁴¹M. Hollstein, D. C. Lorents, and J. R. Peterson, *Bull. Am. Phys. Soc.* **14**, 262 (1969); J. R. Sheridan, J. R. Peterson, M. Hollstein, and D. C. Lorents (unpublished).

⁴²J. O. Hirschfelder, *Intermolecular Forces: Advances in Chemical Physics Vol. 12* (Wiley-Interscience, Inc., New York, 1967), p. 3.

⁴³W. R. Thorson, *J. Chem. Phys.* **34**, 1744 (1961).

⁴⁴W. R. Thorson, *J. Chem. Phys.* **42**, 3878 (1965).

⁴⁵N. F. Mott and H. S. W. Massey, *The Theory of Atomic Collisions* (Oxford University Press, London, 1965), 3rd ed.

⁴⁶K. W. Ford and J. A. Wheeler, *Ann. Phys. (N. Y.)* **7**, 259 (1959).

⁴⁷J. C. Browne, *Phys. Rev.* **138**, A9 (1965); B. K. Gupta and F. A. Matsen (private communication).

⁴⁸D. R. Hartree, *The Calculation of Atomic Structures* (John Wiley & Sons, Inc., New York, 1957), p. 71.

⁴⁹B. K. Gupta and H. H. Michels (private communication).

⁵⁰R. B. Bernstein, in *Molecular Beams: Advances in Chemical Physics*, edited by J. Ross (Wiley-Interscience, Inc., New York, 1966), Vol. X, p. 75.

⁵¹J. VonNeumann and E. Wigner, *Physik. Z.* **30**, 467 (1929).